Numerical Analysis of Hybrid Nanomaterial fluid flow with Dust Particles over a Permeable Vertical Wedge

Nadeem Abbas[a], Wasfi Shatanawi[a,b,c], Kamaleldin Abodayeh[a], Taqi A.M. Shatnawi[c]*

[a]Department of Mathematics and Sciences, College of Humanities and Sciences, Prince Sultan University, Riyadh, 11586, Saudi Arabia

[b]Department of Medical Research, China Medical University Hospital, China Medical University, Taichung, 40402, Taiwan

[c]Department of Mathematics, Faculty of Science, The Hashemite University, P.O Box 330127, Zarqa, 13133, Jordan

Corresponding author:+962799724027, wshatanawi@psu.edu.sa

Abstract

This study investigates the magnetohydrodynamics and fluctuating mixing convection of hybrid nanofluid flows containing dusty fluids in a permeable vertical wedge. A mathematical model based on the concept of fluid flow was developed. The model uses the boundary layer approximation to simplify the partial differential equations. Using appropriate transformations, this set of differential equations is converted into a general system of differential equations. We used the method of obstacles and the bvp4c approach to solve the obtained nonlinear dimensionless differential equations. We worked out to gain results of all values of non dimensional space variable ζ and small values of ζ. The effects of involving physical significant parameters are highlighted by graphs. As the Richardson number increases, both the friction coefficient and the Nusselt number increase. This behavior demonstrates the complex interplay between buoyancy and momentum/heat transfer in the flow. Skin friction and Nusselt number declined due to increasing values of thermal slip (thermal slip). In summary, increased thermal slip affects fluid–solid surface interactions, resulting in lower skin friction (less resistance to fluid flow) and lower Nüssel number (reduced convective heat transfer).

Keywords: Dust particle; Thermal slip; Vertical wedge; Hybrid nanofluid; MHD; Shooting method.

1. Introduction

Saffman [1] was the first one who analyzed the stability of the laminar flow of a dust particle of gas. He derived the momentum equation and temperature equation which satisfy the small disturbance of the steady flow of fluids. After that, many investigators are interested to reveal the impacts of different assumptions on the dusty fluid flow. There are many applications of dusty fluid particle which are used in physiological flow, in purification of crude oil, technological field and so on. Another vital role of the dust particle in boundary layers takes account of soil salvation through natural winds, dust entertainment in a cloud formed in the period of a nuclear explosion and lunar surface erosion through consume of a landing vehicle.

Michael and Miller [2] have been discussed dusty gas particles over plane parallel plates. They discussed two cases in their investigations like as when plate moves along the simple harmonic motion and impulsive rest at uniform velocity. Michael [3] has investigated about the spherical shape of the dusty gas particle with small relaxation time. Marble [4] has analyzed the small particle of dusty gases. He claimed that the cloud particles are governed through four physical parameters which have own significance physically for the gas particle flow systems. Singh and Ram [5] have been highlighted the effects of electrically conducting dusty particles of unsteady flow by channel. The flow of the natural convection of dusty fluid particles of unsteady flow over rectangular channel has been highlighted by Dalal et al. [6]. They investigated different point of views to analyze the heat like as adiabatic horizontal and vertical walls. Time dependent mixed convection flow ovr symmetric wedge investigated by Hossain et al. [7]. Palani and Ganesan [8] have premeditated the heat flow over semi-infinite inclined plate for the dusty fluid. They analyze the heat flow effects on the inclined plate. Ellahi [9] investigates the complex effects of magnetohydrodynamics (MHD) and temperature-dependent viscosity on non-Newtonian nanofluid flow in pipes, providing insightful analytical solutions to understand the fundamental differences governing these complex systems. Khan et al. [10] contributed to this setting by investigating the magnetohydrodynamics of peristaltic flow in a Walther B fluid, considering slip effects and heat transfer. Their work reveals nuances of fluid behavior in peristaltic systems and provides valuable insights into the interplay between magnetohydrodynamics and heat transfer phenomena. Hossain et al. [11] have explored the influence of mixed convection of dusty fluid over a vertical wedge. They discussed about the surface temperature and small fluctuation in free stream. Sheikholeslami et al. [12] deliberated the MHD nanomaterial fluid at permeable surface, applying the decay law numerically. Hasnain et al. [13] highlighted the dusty Casson fluid at permeable sheet under the MHD and power law model. Unsteady of dusty of non Newtonian based Casson fluid over a vertical wedge is discussed by Hady et al. [14]. A study by Yousif et al. [15] focused on the numerical study of momentum and heat transfer of MHD Carreau nanofluids in an exponentially stretched plate by incorporating internal heat source/sink and radiation effects. This study sheds light on the interplay of various factors that affect the behavior of nanofluids in such scenarios. Cattaneo Christov heat flux model based dusty fluid debated by Reddy et al. [16]. Several researchers are interested about the dusty fluid particle with phase flow model having different suppositions (see Refs. [17-19]).

Heat enhancement is the most important problem in the usual life because crisis of energy. Many investigators get attention to resolve this issue. The well known convectional heat transfer fluid like as mineral oil, water and ethylene glycol have low heat transfer because of low thermal conductivity. Choi [20] was the first one who introduced the word Nanofluid. Nanofluid is a type of fluid which consists of solid nanoparticle with base the fluids. There are numerous claims in the fields of engineering, industrial and lubricants. Because of high thermal conductivity. Several methods have been established to enhance the thermal conductivity of these fluids through suspending micro/nano sized particle material in the fluid. Lee et al. [21] was extended the work of Choi [20]. They used the oxide nanoparticle to find out the thermal conductivity. Das et al. [22] highlighted the properties of nanofluids, synthesis, applications and characterization. Mostly used nanosized particles include metal oxides, metal carbides, metal nitride, carbon materials and metals with base fluids like as water, oil and ethylene glycol. Nanofluid gained most of the interest for different purpose by the authors. Haq et al. [23] discussed the micropolar flow of nanofluid over the convective stretching surface under stagnation point region. Ellah et al. [24] reflected the mixed convection of nanofluid flow over permeable wedge. Alamri et al. [25] demonstrated the use of Stefan Blowing to contribute to the understanding of nanofluid behavior under complex flow conditions by investigating the convective-radiative plane flow of nanofluids through porous media with slip effects. Sjah et al. [26] focus on numerical simulations of magnetohydrodynamic nanofluids in porous media, emphasizing the effects of form factor and heat transfer. Their research uses computational methods to investigate how these factors affect the behavior of nanofluids in porous media, contributing to a deeper understanding of complex systems. Several researchers are interested to gain different results for various assumptions which see in Refs. [27-29].

Heat transfer enhancement is important in real life because of its vital consumptions of technology and engineering fields. Most of the interest of researchers focuses on the heat transfer augmentation. The word Hybrid nanofluid introduced by Suresh et al. [30]. Hybrid nanofluid is a type of fluid which consist of two different nanosized particles with base fluid. They claimed that hybrid nanofluid gains higher heat transfer than that of simple nanofluid. Labib et al. [31] emphasized the impacts of hybrid nanofluid experimentally. Sundar and Sousa [32] discussed the hybrid nanomaterial liquid under the turbulent flow. They studied the heat transfer improvement of low volume concentration of hybrid nanofluids. Nadeem et al. [33] explored the hybrid nanomaterial liquid at circular cylinder. Nadeem and Abbas [34] premeditated the microploar hybrid nanomaterial liquid flow over a circular cylinder with slip

conditions. Sheikholeslami et al. [35] explored the turbulent convect nanofluid flow in a circular duct. Dalkılıç et al. [36] has investigated the hybrid nanomaterial liquid flow experimentally in horizontal tube. Hybrid nanofluid flow at channel has analyzed by Sheikholeslami et al. [37]. According to references [38–41], a number of scientists are investigating the heat transmission of hybrid nanomaterial liquids under numerous physical hypotheses.

In the reviewed literature, research focuses on the flow of hybrid nanomaterial fluids through vertical plates, combining magnetohydrodynamic and dust-fluid phenomena. A mathematical model based on the principles of fluid flow was developed. The incomplete differential (PDEs) equations were converted to a system of ordinary differential equations (ODEs) using an appropriate similarity transformation. These dimensionless nonlinear equations were solved computationally using the BVP4C method in addition to perturbation theory. The resulting solutions were carefully analyzed based on various physical properties.

2 Mathematical formulations

In the presence of solid nanoparticles, consider the hybrid nanomaterial liquid with mixed convection fluctuating having dusty particles over a vertical wedge. Fig. 1 shows the coordinate system and flow setup. The thermal thickness is δ_M and momentum thickness is δ_T. It is expected that the free stream and surface temperatures oscillate in time with tiny amplitudes around a stable, non-zero mean free stream velocity. The system of mathematics has been taken into consideration as follows using the supposition and standard approximationof boundary layer [see Refs. 11, 38, 40, 41]:

$$\frac{\partial v}{\partial x}+\frac{\partial w}{\partial y}=0, \tag{1}$$

$$w\frac{\partial v}{\partial y}+\frac{\partial v}{\partial t}+v\frac{\partial v}{\partial x}=-\frac{\partial p}{\partial x}+\left(\frac{\mu_{hnf}}{\rho_{hnf}}\right)\frac{\partial^2 v}{\partial^2 y}+\frac{\rho_f g\beta\cos\left(\pi/4\right)T}{\rho_{hnf}}+\frac{\rho_p}{\rho_{hnf}\tau_m}\left(v_p-v\right)-\frac{\sigma B_\infty^2}{\rho_{nf}}v-\frac{\mu_f}{k_0}v, \tag{2}$$

$$\left(w\frac{\partial T}{\partial x}+\frac{\partial T}{\partial t}+v\frac{\partial T}{\partial x}\right)=\alpha_{hnf}\frac{\partial^2 T}{\partial y^2}-\frac{\rho_p c_S}{\tau_T}\left(T_p-\bar{T}\right), \tag{3}$$

$$\frac{\partial v_P}{\partial x}+\frac{\partial w_P}{\partial y}=0, \tag{4}$$

$$\rho_p\left(\frac{\partial v_p}{\partial t}+v_p\frac{\partial v_p}{\partial x}+w_P\frac{\partial v_p}{\partial y}\right)=-\frac{\rho_p}{\tau_m}\left(v_p-v\right), \tag{5}$$

(6)

Where, $\bar{T}=T-T_\infty$, the BC

$$v=v_P=\lambda_3\frac{\partial v}{\partial y},\ w_P=w=0,\bar{T}=T_P=\lambda_0\kappa_{hnf}\frac{\partial T}{\partial y}+T_W,\ \ at\ \ y\to 0,$$
$$\bar{T}=T_P=0,v\to v_e\left(x,t\right),\ \ at\ \ \ y\to\infty. \tag{7}$$

The volumetric coefficient communication for temperature is β, $v_e\left(x,t\right)$ be the velocity of free stream, w and v are the local velocity factors of the fluid, ρ_{hnf} (density), μ_{hnf} (viscosity), α_{hnf} (thermal conductivity) and ρC_{phnf} (heat capacity) of hybrid nanofluid. ρ_p is the density of the particle (cloud deformation of underform able) with a single radius R. Such particle (cloud) is also defined as a set of continuum variable v_p, w_p and T_p. The heat capacity of fluid and dust particle at fix pressure are C_p and C_s. $N_p\mathrm{M}=\rho_p$, here the local number of the particle per unit volume and mass of particle is defined as N_p and M. The characteristic of the time is presented as τ_m. This is a given time to require by the particle to decline the velocity of particle (fluid) relative to the liquid through $e^{(-1)}$ of its original values in the un-accelerated state. This velocity equilibration time contributes few indication of the gas particle interaction procedure when compared to the time τ symbolizing the flow. When $\tau\gg\tau_m$, the particle adjusts to the local gas velocity before, it has transferred by a significant portion of the region. The cloud particle would consider the uniform velocity very quickly, if the velocity of gas was uniform. The velocity of particle depend highly on the fluid motion which inversely dependent of its prior history. Moreover, τ_T is presented in Eqs. (3) and (6) and defined as $\tau_T=\frac{MC_s}{6\pi\mu R}$. This is a given time to require for the temperature variation between a gas and particle to be decline to $e^{(-1)}$ of its initial values. If the $\tau_T=\frac{MC_s}{6\pi\mu R}\gg 1$, then the particle is independent of the local gas particle but strongly related to its initial

values. If $\tau_T = \frac{MC_s}{6\pi\mu R} \ll 1$, then the temperature of the particle is expressed highly through local conditions. The limiting form of the coupled equations of the system of gas particle which is useful analytically as well as physically. We want to discuss about τ_T and τ_m when τ_T and τ_m become very small, the local particle temperature and particle slip velocity become small. Consider the above approximation, the number of the dependent variable decreases by two such that $T_p = T$, $\left(v_p, w_p\right) = \left(v, w\right)$. It is easy to found that $v_p \to v$ and $w_p \to w \Rightarrow D\left(\frac{\rho_p}{\rho}\right) = \text{constant}$, this relation shows that the particle is to be fixed to the mass of gas in which they were originally located. If the initial distribution of the particles is uniformly, so the entire medium is constant like as $\frac{\rho_p}{\rho_f} = K$. Using the above suppositions, the system become as:

$$\frac{\partial v}{\partial x} + \frac{\partial w}{\partial y} = 0, \tag{8}$$

$$\frac{\partial v}{\partial t} + v\frac{\partial v}{\partial x} + w\frac{\partial v}{\partial y} = \frac{\partial v_0}{\partial t} + v_0\frac{\partial v_0}{\partial x} + \frac{g\beta\cos\left(\pi/4\right)\bar{T}}{\rho_{hnf}\left(1+K\right)} + \left(\frac{\nu_{hnf}}{1+K}\right)\frac{\partial^2 v}{\partial y^2} - \left(\frac{\sigma B_\infty^2}{\rho_{hnf}\left(1+K\right)}\right)v - \left(\frac{\nu_f}{\rho_{hnf}\left(1+K\right)k_0}\right)v, \tag{9}$$

$$\left(\frac{\partial \bar{T}}{\partial t} + v\frac{\partial \bar{T}}{\partial x} + w\frac{\partial \bar{T}}{\partial y}\right) = \frac{\alpha_{hnf}}{\left(1+\xi K\right)}\frac{\partial^2 \bar{T}}{\partial y^2}, \tag{10}$$

With BC

$$\begin{gathered} w = 0,\ v = \lambda_3\frac{\partial v}{\partial y},\quad \bar{T} = \kappa_{hnf}\lambda_0\frac{\partial \bar{T}}{\partial y} + T_W,\ \ at\ \ y \to 0. \\ v \to v_w\left(x,t\right),\ \ \bar{T} = 0,\ \ at\ \ \ y \to \infty, \end{gathered} \tag{11}$$

Where

$$v_w\left(x,t\right) = v_w\left(x\right)\left[1+\epsilon\cos\left(\omega t\right)\right] \text{ and } T_W\left(x,t\right) = \bar{T}_w\left(x\right)\left[1+\epsilon\cos\left(\omega t\right)\right]. \tag{12}$$

The mean surface temperature is $\bar{\mathrm{T}}_0\left(\mathrm{x}\right)$ and velocity is $\mathrm{V}_0\left(\mathrm{x}\right)$, and amplitude of oscillation is ϵ which is $\epsilon \ll 1$ while the ω is oscillation frequency. Table 1 presented the thermodynamics charactristics of nanoparticles and base fluid.

The hybrid nanofluid's thermal characteristics and their expressions are described as follows:

Properties	Hybrid Nanofluid

Density $\rho_{hnf} = \Phi_1\rho_{s_1} + \Phi_2\rho_{s_2} + (1-\Phi_2)(1-\Phi_1)\rho_f.$

Heat capacity $\left(\rho C_p\right)_{hnf} = \Phi_1\left(\rho C_p\right)_{s_1} + \Phi_2\left(\rho C_p\right)_{s_2} + (1-\Phi_2)(1-\Phi_1)\rho_f.$

Dynamics Viscosity $\mu_{hnf} = \dfrac{\mu_f}{(1-\Phi_2)^{5/2}(1-\Phi_1)^{5/2}}.$

Thermal conductivity of Yamada-Ota Model

$$\frac{k_{bf}}{k_f} = \frac{1+\dfrac{k_f}{k_{s_1}}\dfrac{L}{R}+\left(1-\dfrac{k_f}{k_{s_1}}\right)\dfrac{L}{R}+2\left(\dfrac{k_{s_1}}{k_{s_1}-k_f}\right)\ln\left(\dfrac{k_{s_1}+k_f}{2k_{s_1}}\right)}{1-+2\phi_2\left(\dfrac{k_f}{k_{s_1}-k_f}\right)\ln\left(\dfrac{k_{s_1}+k_f}{2k_f}\right)},$$

$$\frac{k_{hnf}}{k_{bf}} = \frac{1+\dfrac{k_{bf}}{k_{s_2}}\dfrac{L}{R}\phi_2^{\,0.2}+\left(1-\dfrac{k_{bf}}{k_{s_2}}\right)\phi_2\dfrac{L}{R}\phi_2^{\,0.2}+2\phi_2\left(\dfrac{k_{s_2}}{k_{s_2}-k_{bf}}\right)\ln\left(\dfrac{k_{s_2}+k_{bf}}{2k_{s_2}}\right)}{1-\phi_2+2\phi_2\left(\dfrac{k_{bf}}{k_{s_2}-k_{bf}}\right)\ln\left(\dfrac{k_{s_1}+k_f}{2k_{s_1}}\right)}.$$

3 Solution procedure

In order to consider solutions to Eqs. (9–11) for the boundary conditions stated in Eq. (12), take the following form

$$v(x,y,t) = \epsilon\exp(\omega it)v_2 + v_1, \tag{13}$$

$$w(x,y,t) = \epsilon\exp(\omega it)w_2 + w_1, \tag{14}$$

$$\bar{T}(x,y,t) = \epsilon\exp(\omega it)T_2 + T_1. \tag{15}$$

The fluctuating quantities are $\mathrm{v}_1, \mathrm{v}_2$ and velocity factors are $\mathrm{w}_1, \mathrm{w}_2$. The real (v, w) and fluctuating (T_1, T_2) part of the T (temperature function). The actual components of the functions identified in Equation are the predicted solution functions (13). We obtained succeeding equations by applying the Eqs. (13) in Eqs. (9–12) and changing the terms and conditions to $0(\epsilon)$.

$$\frac{\partial \mathrm{w}_1}{\partial \mathrm{y}} + \frac{\partial \mathrm{v}_1}{\partial \mathrm{x}} = 0, \tag{16}$$

$$\mathrm{w}_1\frac{\partial \mathrm{V}_1}{\partial \mathrm{Y}} + \mathrm{V}_1\frac{\partial \mathrm{V}_1}{\partial \mathrm{X}} = \mathrm{V}_\mathrm{w}\frac{\partial \mathrm{V}_\mathrm{w}}{\partial \mathrm{X}} + \frac{\partial^2 \mathrm{V}_1}{\partial^2 \mathrm{Y}}\left(\frac{\nu_{\mathrm{hnf}}}{1+\mathrm{K}}\right) + \frac{\mathrm{g}\beta\cos\left(\pi/4\right)\mathrm{T}_1}{\rho_{\mathrm{hnf}}(1+\mathrm{K})} - \left(\frac{\sigma \mathrm{B}_\circ^2}{\rho_{\mathrm{hnf}}(1+\mathrm{K})}\right)\mathrm{v}_1 - \left(\frac{\nu_\mathrm{f}}{\rho_{\mathrm{hnf}}(1+\mathrm{K})\mathrm{k}_0}\right)\mathrm{v}_1, \tag{17}$$

$$\frac{\partial \Psi_1}{\partial \mathrm{y}}\frac{\partial \mathrm{T}_1}{\partial \mathrm{x}} - \frac{\partial \Psi_1}{\partial \mathrm{x}}\frac{\partial \mathrm{T}_1}{\partial \mathrm{y}} = \frac{\alpha_{\mathrm{hnf}}}{(1+\xi\mathrm{K})}\frac{\partial^2 \mathrm{T}_1}{\partial \mathrm{y}^2}. \tag{18}$$

Having BC

$$w_1 = 0,\ \ v_1 = \lambda_3 \frac{\partial v_1}{\partial y},\ \ \ T_1 = \bar{T}_0(x) + \lambda_0 \kappa_{hnf} \frac{\partial T_1}{\partial y},\ \ at\ \ y \to 0,$$

$$v_1 \to v_0(x,t),\ \ T_1 = 0,\ \ at\ \ \ y \to \infty. \tag{19}$$

And

$$\frac{\partial v_2}{\partial x} + \frac{\partial w_2}{\partial y} = 0, \tag{20}$$

$$i\omega t v_2 + v_1 \frac{\partial v_2}{\partial x} + w_1 \frac{\partial v_2}{\partial y} + v_2 \frac{\partial v_1}{\partial x} + w_2 \frac{\partial v_1}{\partial y} = \omega i t v_w(x) + v_0 \frac{\partial v_0}{\partial x} + \left(\frac{\nu_{hnf}}{1+K}\right)\frac{\partial^2 v_2}{\partial y^2}$$
$$+ \frac{g\beta \cos\left(\pi/4\right) T_2}{\rho_{hnf}(1+K)} - \left(\frac{1}{\rho_{hnf}(1+K)}\right)\frac{\sigma B_\circ^2}{\rho_{nf}} v_2 - \left(\frac{\nu_f}{\rho_{hnf}(1+K)k_0}\right) v_2, \tag{21}$$

$$v_1 \frac{\partial T_2}{\partial x} + \omega i t T_2 + V_2 \frac{\partial T_1}{\partial x} + w_2 \frac{\partial T_1}{\partial y} + w_1 \frac{\partial T_2}{\partial y} = \frac{\alpha_{hnf}}{(1+\xi K)} \frac{\partial^2 T_2}{\partial y^2}. \tag{22}$$

Having BC

$$w = 0,\ \ v_2 = \lambda_3 \frac{\partial v_2}{\partial y},\ \ T_2 = \kappa_{hnf} \lambda_0 \frac{\partial T_2}{\partial y} + \bar{T}_0(x),\ \ at\ \ y \to 0,$$

$$T_2 = 0,\ v_2 = v_0(x),\quad at\ \ \ y \to \infty. \tag{23}$$

The functions $v_0(\mathrm{x})$ and $\bar{T}_0(x)$ like as $v_c x^{1/2} = \mathrm{v}_0(\mathrm{x})$ and $T_c = \bar{T}_0(x)$ while v_c, T_c are the constants. Now, we introduced as

$$\Psi_1 = \nu_f x \sqrt{Re_x}(1+Pr)^{-3/4} f(\eta),\ T_1 = T_w \Theta(\eta),$$
$$\Psi_2 = \nu_f x \sqrt{Re_x}(1+Pr)^{-3/4} g(\eta,\zeta),\ T_2 = T_w h(\eta,\zeta), \tag{24}$$
$$\eta = y\sqrt{Re_x}(1+Pr)^{1/4},\ \ \zeta = \frac{\omega}{\mathrm{v}_c}\sqrt{x}.$$

The Ψ_1, Ψ_2 are stream functions which fulfill the Eqs. (14) and (18) respectively. The similarity is η and local frequency is ζ. We obtain the dimensionless form by relating the alteration Eq. (23) to Eqs. (20) and (22):

$$\frac{Pr+1}{(K+1)} \mathrm{v}_{\mathrm{hnf}} f''' + 3/4\, f f'' - \frac{1}{2}(f f' - \mathrm{Pr} - 1) + \frac{\rho_f Ri}{\rho_{\mathrm{hnf}}} \frac{Pr+1}{(1+K)} \Theta - \frac{1+Pr}{(1+K)} \frac{\rho_f M}{\rho_{\mathrm{hnf}}} f' - \frac{1+Pr}{(1+K)} \frac{\rho_f \lambda_1}{\rho_{\mathrm{hnf}}} f' = 0, \tag{25}$$

$$\frac{1+Pr}{Pr(1+K\xi)} \alpha_{\mathrm{hnf}} \Theta'' + 3/4\, f \Theta' = 0. \tag{26}$$

$$f(\eta)=0,\ f'(\eta)=\lambda\frac{\mu_{hnf}}{\mu_f}(1+Pr)^{\frac{1}{2}}\ f''(\eta),$$
$$\Theta(\eta)=1+\gamma\frac{\kappa_{hnf}}{\kappa_f}(1+Pr)^{1/4}\Theta'(\eta),\ \eta\to 0, \tag{27}$$
$$f'(\eta)\to(1+\mathrm{Pr})^{1/2},\ \Theta(\eta)\to 0, as\ \eta\to\infty.$$

The part of steady as

$$\frac{1+Pr}{(1+K)}\nu_{hnf}g'''+\frac{3}{4}(fg''+f''g)-f'g'+i\zeta\left\{Pr+1-(\mathrm{Pr}+1)^{\frac{1}{2}}g'\right\}+1+\mathrm{Pr}+$$
$$\frac{\rho_f Ri}{\rho_{hnf}}\frac{1+Pr}{(1+K)}h-\frac{1+Pr}{(1+K)}\frac{\rho_f M}{\rho_{hnf}}g'-\frac{1+Pr}{(1+K)}\frac{\rho_f\lambda_1}{\rho_{hnf}}g'=\frac{1}{2}\zeta\left(f'\frac{\partial g'}{\partial\xi}-f''\frac{\partial g}{\partial\xi}\right), \tag{28}$$

$$\frac{1+Pr}{Pr(1+K\xi)}\alpha_{hnf}h''+\frac{3}{4}(fh'+\Theta' g)-i\zeta(1+\mathrm{Pr})^{\frac{1}{2}}h=\frac{1}{2}\zeta\left(f'\frac{\partial h}{\partial\xi}-\Theta'\frac{\partial g}{\partial\xi}\right), \tag{29}$$

having conditions are

$$g(\eta)=0,\ g'(\eta)=\lambda\frac{\mu_{hnf}}{\mu_f}(Pr+1)^{\frac{1}{2}}g''(\eta),$$
$$h(\eta)=1+\gamma\frac{\kappa_{hnf}}{\kappa_f}(1+Pr)^{1/4}h'(\eta),\ \eta\to 0, \tag{30}$$
$$g'(\eta)\to(1+Pr)^{1/2},\ h(\eta)\to 0, as\ \eta\to\infty.$$

4 Perturbation solutions for small ζ

The outcomes based on the series' finite number of terms are only applicable for a narrow frequency range in order to capture the effects of mixed convection close to the leading edge. So

(31)

Putting these values in Eqs. (28-29), then equating the coefficients of $(2i\zeta)^0$

$$\frac{1+Pr}{(1+K)}\nu_{hnf}g_0'''+\frac{3}{4}(fg_0''+f''g_0)-f'g_0'+1+\mathrm{Pr}+\frac{\rho_f Ri}{\rho_{hnf}}\frac{1+Pr}{(1+K)}h_0-\frac{1+Pr}{(1+K)}\frac{\rho_f M}{\rho_{hnf}}g_0'-\frac{1+Pr}{(1+K)}\frac{\rho_f\lambda_1}{\rho_{hnf}}g_0'=0, \tag{32}$$

$$\frac{1+Pr}{Pr(1+K\xi)}\alpha_{hnf}h_0''+\frac{3}{4}(fh_0'+\Theta' g_0)=0, \tag{33}$$

respected boundary conditions are

$$g_0(\eta)=0,\ g_0'(\eta)=\lambda\frac{\mu_{hnf}}{\mu_f}(1+Pr)^{\frac{1}{2}}g_0''(\eta),$$
$$h_0(\eta)=1+\gamma\frac{\kappa_{hnf}}{\kappa_f}(1+Pr)^{1/4}h_0'(\eta),\ \ \eta\to 0, \tag{34}$$
$$g_0'(\eta)\to(1+Pr)^{1/2},\ \ h_0(\eta)\to 0, as\,\eta\to\infty.$$

Equating the coefficients of $(2i\zeta)^1$

$$\frac{1+Pr}{(1+K)}\nu_{hnf}g_1'''+\tfrac{3}{4}fg''+\tfrac{5}{4}f''g_1-\tfrac{3}{2}f'g_1'-\frac{1+Pr}{(1+K)}\frac{\rho_f M}{\rho_{hnf}}g_1'-$$
$$\frac{1+Pr}{(1+K)}\frac{\lambda_1\rho_f}{\rho_{hnf}}g_1'+\frac{\rho_f Ri}{\rho_{hnf}}\frac{Pr+1}{(K+1)}h_1+\tfrac{1}{2}(1+\Pr)-\tfrac{1}{2}(1+\Pr)^{\frac{1}{2}}g_0'=0, \tag{35}$$

$$\frac{1+Pr}{\Pr(1+K\xi)}\alpha_{hnf}h_1''+\tfrac{3}{4}fh'+\tfrac{5}{4}\Theta'g_1-\tfrac{1}{2}f'h_1-\tfrac{1}{2}(1+\Pr)^{\frac{1}{2}}h_0=0. \tag{36}$$

Having BC

$$g_1(\eta)=0,\ g_1'(\eta)=\lambda\frac{\mu_{hnf}}{\mu_f}(Pr+1)^{\frac{1}{2}}g_1''(\eta),$$
$$h_1(\eta)=\gamma\frac{\kappa_{hnf}}{\kappa_f}(Pr+1)^{1/4}h_1'(\eta),\ \ \eta\to 0, \tag{37}$$
$$g_1'(\eta)\to 0,\ \ h_1(\eta)\to 0, as\,\eta\to\infty.$$

Equating the coefficients of $(2i\zeta)^n$

$$\frac{1+Pr}{(1+K)}\nu_{hnf}g_n'''+\tfrac{3}{4}fg_n''+\left\{\tfrac{3}{4}+\tfrac{n}{2}\right\}f''g_n-\left\{1+\tfrac{n}{2}\right\}f'g_n'-\frac{1+Pr}{(1+K)}\frac{\rho_f M}{\rho_{hnf}}g_n'-$$
$$\frac{1+Pr}{(1+K)}\frac{\lambda_1\rho_f}{\rho_{hnf}}g_n'+\frac{\rho_f Ri}{\rho_{hnf}}\frac{1+Pr}{(1+K)}h_n-\tfrac{1}{2}(1+\Pr)^{\frac{1}{2}}g_{n-1}'=0, \tag{38}$$

$$\frac{1+Pr}{\Pr(1+K\xi)}\alpha_{hnf}h_n''+\tfrac{3}{4}fh_n'+\left\{\tfrac{3}{4}+\tfrac{n}{2}\right\}\Theta'g_n-\tfrac{1}{2}f'h_n-\tfrac{1}{2}(1+\Pr)^{\frac{1}{2}}h_{n-1}=0. \tag{39}$$

Having BC

$$g_n(\eta)=0,\ g_n'(\eta)=\lambda\frac{\mu_{hnf}}{\mu_f}(1+Pr)^{\frac{1}{2}}g_n(\eta),$$
$$h_n(\eta)=\gamma\frac{\kappa_{hnf}}{\kappa_f}(1+Pr)^{1/4}h_n'(\eta),\ \ \eta\to 0, \tag{40}$$
$$g_n'(\eta)\to 0,\ \ h_n(\eta)\to 0,\ \ as\,\eta\to\infty.$$

The physical feature of boundary layer flow presented. The Nusselt number represents the improvement of convective heat transfer over conductive heat transfer and is defined

$Nu = \dfrac{q_w(x)\,x}{k_f\left(T_w - T_\infty\right)}$. Where, the coefficient of surface friction for flow over a plate can be described by the following equation using the concepts of local shear stress and dynamic viscosity $C_f = \dfrac{\tau_w(x)}{\rho_f u_e(x)^2}$. The dimensionless quatities become

$$\text{Skin friction} = \frac{\mu_{hnf}}{\mu_f}(1+Pr)^{-\frac{1}{4}}(\zeta)^{-\frac{1}{2}}\, g''(\xi,0) = \sum_{n=0}^{\infty}(2i\zeta)^{n-\frac{1}{2}}\, g_n^{"}(0),$$

$$\text{Nusselt number} = \frac{\kappa_{hnf}}{\kappa_f}(1+Pr)^{-\frac{1}{4}}(\zeta)^{-\frac{1}{2}}\, h'(\xi,0) = \sum_{n=0}^{\infty}(2i\zeta)^{n-\frac{1}{2}}\, h_n^{'}(0).$$

5 Result and discussions

In the present analysis, the authors have investigated the hybrid nanofluid fluid flow over a vertical wedge with velocity and thermal slip effects. Mathematical model have settled as partial differential equations through the Navier–Stokes equations. The above system of partial differential equations changed into ordinary differential equations. Transformed systems of equations have been elucidated by the numerical scheme (BVP4C) and perturbation method for low frequency range. Significant results have been gained and plotted through graphs for the different physical parameters. Table 2 debated the physical phenomena features on the skin friction and Nusselt number. Nusselt number reduced due to increasing values of nano concentration while friction of fluid increased due to increasing in nano concentration factor. Due to the high nanoconcentration, the friction properties of the liquid on the vertical wedge increase. The interaction between the nanoparticles and the fluid tends to increase the overall viscosity and, consequently, the frictional force acting on the surface of the wedge. This increased friction can affect fluid flow patterns, altering the behavior of the boundary layer and flow separation at the wedge surface. As the Richardson number increases, both the friction coefficient and the Nusselt number increase. This behavior demonstrates the complex interplay between buoyancy and momentum/heat transfer in the flow. An increase in the coefficient of friction means an increase in the resistance to the flow of the fluid on the surface of the wedge. Under the influence of a strong magnetic field, the hybrid nanofluid undergoes altered flow, which can lead to increased shear stress and increased resistance to movement along the wedge surface due to magnetic forces acting on the nanoparticles and the carrier fluid. The porous structure promotes better mixing and interaction between the fluid and solid matrix, making convective heat transfer more efficient. Therefore, even though the frictional resistance increases, the convective heat

transfer within the boundary layer is enhanced and the Nusselt number increases. The ξ increased which declined the skin friction and increased the Nusselt number. Skin friction and Nusselt number declined due to increasing values of thermal slip slip (momentum slip). In summary, increased thermal slip affects fluid–solid surface interactions, resulting in lower skin friction (less resistance to fluid flow) and lower Nüssel number (reduced convective heat transfer). Skin friction and Nusselt number declined due to increasing values of velocity slip (momentum slip). The relative velocity between the fluid and the solid surface increases, reducing skin friction because the fluid experiences less resistance or friction from the surface. The Nusselt number decreases because the altered flow dynamics and near-surface velocity profile result in reduced convective heat transfer, resulting in a lower Nusselt number. The K increased which enhanced the skin friction and the Nusselt number. The ζ increased which declined the skin friction and the Nusselt number. Figs. 2-3 reported the influence of steady case and unsteady case using different order for temperature function and analyzed the influnec of physical paramters namely: solid nano concentration and thermal slip. The temparture increased due to higher values of solid nano concentration which reported in Fig. 2 for all case of steady and unsteady. The temparture reduced due to higher values of solid nano concentration which reported in Fig. 3 for all case of steady and unsteady. Fig. 4 reveals the impacts of Φ_2 on the skin friction for various values of M for small and all values of ζ. It is perceived that when the values of Φ_2 Increases with declining skin friction for both cases, small and all values of ζ. The skin friction increases with enhancing in M for small values of ζ while declines for large values of M in case of all values of ζ. Fig. 5 exhibits the effects of M and Φ_2 in both cases for small and all values of ζ. It is seen that the Nusselt number decays for large values of M and Φ_2 for both cases for small and all values of ζ. A significant result gains which we observed, small values of ζ get decline curved as compared to all values of ξ. Fig. 6 shows the impacts on the Nusselt number and skin frictions for the dissimilar values of λ. It is seen that the skin friction decays for higher values of λ while decays for larger values of ζ. The impacts of λ on the Nusselt number and skin frictions which exhibit in Fig. 6. It is perceived that Nusselt number rises for the greater values of λ but opposite trend is seen to be noted for greater values of ζ. Fig. 7 exhibits the influence of on the Nusselt number and skin friction. It is observed that Skin friction and Nussslt number decline for large values of K while opposite seen for the large values of ζ. Table 3 presented the variation of skin friction of current analysis with

Hossain et al. [11] when $Pr = 0.72, Ri = 4.0, K = 0.0, \chi = 1.0, \lambda = 0.0, \gamma = 0.0, M = 0.0, \lambda_1 = 0.0, \Phi_1 = \Phi_2 = 0.0$. It is noted that our results are good agreement with Hossain et al. [11].

6 Final Remarks

We investigated the unsteady mixed convection of a two-dimensional hybrid nanofluid flowing over a vertical wedge, considering the influence of slip and magnetic fields. Our study included analyzing the impact of slight fluctuations in surface temperature and free stream. We comprehensively examined the effects of significant physical parameters liike as thermal slip, velocity slip, magnetic field, solid nanoparticles, Richardson number, and K dimensional parameter on skin friction and Nusselt number across the frequency spectrum in this analysis. Few main points are presented as:

- As the Richardson number increases, both the friction coefficient and the Nusselt number increase. This behavior demonstrates the complex interplay between buoyancy and momentum/heat transfer in the flow.
- Skin friction and Nusselt number declined due to increasing values of thermal slip slip (thermal slip). In summary, increased thermal slip affects fluid–solid surface interactions, resulting in lower skin friction (less resistance to fluid flow) and lower Nüssel number (reduced convective heat transfer).
- Skin friction and Nusselt number declined due to increasing values of velocity slip (momentum slip). The relative velocity between the fluid and the solid surface increases, reducing skin friction because the fluid experiences less resistance or friction from the surface. The Nusselt number decreases because the altered flow dynamics and near-surface velocity profile result in reduced convective heat transfer, resulting in a lower Nusselt number.
- The Nusselt number decays for large values of M and Φ_2 for both cases for small and all values of ζ. A significant result gains which we observed, small values of ζ get decline curved as compared to all values of ζ.

Acknowledgement: Authors would like to thank Prince Sultan University for their support through the TAS research lab.

References

1 Saffman, P. G. ‘‘On the stability of laminar flow of a dusty gas’’. *J. Fluid Mech. 1962;**13**(1):120-128*.

2 Michael, D. H. and Miller D. A. ‘‘Plane parallel flow of a dusty gas’’. *Mathematika. 1966;**13**(1):97-109*.

3 Michael, D. H. ‘‘The steady motion of a sphere in a dusty gas’’. *J. Fluid Mech. 1968;31(1):175-192*.

4 Marble, F. E. ‘‘Dynamics of dusty gases’’. *Annu. Rev. Fluid Mech. 1970;**2**(1):397-446.*

5 Singh, C. B. and Ram, P. C. ‘‘Unsteady flow of an electrically conducting dusty viscous liquid through a channel’’. Indian *J. Pure Appl. Math. 1977;**8**(9):1022-1028*.

6 Dalal, D. C. Datta N., Mukherjea S. K. ‘‘Unsteady natural convection of a dusty fluid in an infinite rectangular channel’’. *Int. J. Heat Mass Transfer. 1998;**41**(3):547-562*.

7 Hossain, M. A., Bhowmick, S. and Gorla, R. S. R. ‘‘Unsteady mixed-convection boundary layer flow along a symmetric wedge with variable surface temperature’’. *Int J Eng Sci. 2006;**44**(10):607-620*.

8 Palani, G., Ganesan, P. ‘‘Heat transfer effects on dusty gas flow past a semi-infinite inclined plate’’. *Forsch Ingenieurwes. 2007;**71**(3-4):223-230*.

9 Ellahi, R. ‘‘The effects of MHD and temperature dependent viscosity on the flow of non-Newtonian nanofluid in a pipe: analytical solutions’’. *Appl Math Model. 2013;**37**(3):1451-1467*.

10 Khan A. A., Usman H, Vafai K, et al. ‘‘Study of peristaltic flow of magnetohydrodynamics Walter's B fluid with slip and heat transfer’’. *Sci Iran. 2016;**23**(6):2650-2662*.

11 Hossain, M. A., Roy, N. C., Siddiqa, S. ‘‘Unsteady mixed convection dusty fluid flow past a vertical wedge due to small fluctuation in free stream and surface temperature’’. *Appl Math Comput. 2017;**293**:480-492.*

12 Sheikholeslami, M., Shehzad, S. A., Li, Z., et al. ‘‘Numerical modeling for alumina nanofluid magnetohydrodynamic convective heat transfer in a permeable medium using Darcy law’’. *Int J Heat Mass Transfer. 2018;**127**:614-622.*

13 Hasnain, J., Abbas, Z., Sheikh, M., et al. ‘‘Analysis of dusty Casson fluid flow past a permeable stretching sheet bearing power law temperature and magnetic field’’. *Int J Numer Meth Heat Fluid Flow. 2019, **30**(6).*

14 Hady, F. M., Mahdy, A., Mohamed, R. A., et al. ‘‘Unsteady natural convection flow of a dusty non-Newtonian Casson fluid along a vertical wavy plate: numerical approach’’. *J Braz Soc Mech Sci Eng. 2019;**41**(11):472.*

15 Yousif, M. A., Ismael, H. F., Abbas, T., et al. ‘‘Numerical study of momentum and heat transfer of MHD Carreau nanofluid over an exponentially stretched plate with internal heat source/sink and radiation’’. *Heat Transf Res. 2019;**50**(7).*

16 Reddy, M. G., Rani, M. S., Kumar, K. G., et al. ‘‘Hybrid dusty fluid flow through a Cattaneo Christov heat flux model’’. *Physica A: Stat Mech Appl. 2020; **551**:123975*.

17 Turkyilmazoglu, M. ‘‘Suspension of dust particles over a stretchable rotating disk and two-phase heat transfer’’. *Int J Multiphase Flow. 2020; **127**:103260*.

18 Nguyen, T. K, Sheikholeslami, M., Jafaryar, M., et al. ‘‘Design of heat exchanger with combined turbulator’’. *J Therm Anal Calorim. 2020;**139**(1):649-659*.

19 Khan, A. A., Arshad, A., Ellahi, R., et al. ‘‘Heat transmission in Darcy-Forchheimer flow of Sutterby nanofluid containing gyrotactic microorganisms’’. *Int J Numer Meth Heat Fluid Flow. 2023;**33**(1):135-152.*

20 Choi, S. U., Eastman, J. A. Enhancing thermal conductivity of fluids with nanoparticles *(No. ANL/MSD/CP-84938; CONF-951135-29). Argonne Natl Lab, IL (United States); 1995.*

21 Lee, S., Choi, S. S., Li, S. A., et al., ‘‘Measuring thermal conductivity of fluids containing oxide nanoparticles’’. *J Heat Transfer. 1999;**12**1(2):280-289*.

22 Das, S. K., Choi, S. U., Yu, W., et al. ‘‘*Nanofluids: science and technology*’’. John Wiley & Sons; 2007.

23 Haq, R. U., Nadeem, S., Akbar, N. S., et al. ‘‘Buoyancy and radiation effect on stagnation point flow of micropolar nanofluid along a vertically convective stretching surface’’. *IEEE Trans Nanotechnol. 2015;**14**(1):42-50.*

24 Ellahi, R., Hassan, M., Zeeshan, A. ‘‘Aggregation effects on water base Al2O3—nanofluid over permeable wedge in mixed convection’’. *Asia-Pacific J Chem Eng. 2016;**11**(2):179-186.*

25 Alamri, S. Z., Ellahi, R., Shehzad, N., et al. ‘‘Convective radiative plane Poiseuille flow of nanofluid through porous medium with slip: an application of Stefan blowing’’. *J Mol Liquids. 2019;**273**:292-304.*

26 Shah, Z., Babazadeh, H., Kumam, P., et al. ‘‘Numerical simulation of magnetohydrodynamic nanofluids under the influence of shape factor and thermal transport in a porous media using CVFEM’’. Front Phys. 2019;**7**:164.

27 Asifa, Anwar T., Kumam, P., et al. ‘‘Significance of shape factor in heat transfer performance of molybdenum-disulfide nanofluid in multiple flow situations; A comparative fractional study’’. *Molecules. 2021;**26**(12):3711.*

28 Zeeshan, A., Ahmad, M., Ellahi, R., et al. ‘‘Hydromagnetic flow of two immiscible nanofluids under the combined effects of Ohmic and viscous dissipation between two parallel moving plates’’. *J Magn Magn Mater. 2023;**575**:170741.*

29 Shah, Z., Shafiq, A., Rooman, M., et al. ‘‘Darcy Forchheimer Prandtl-Eyring nanofluid flow with variable heat transfer and entropy generation using Cattaneo-Christov heat flux model: Statistical approach’’. *Case Stud Thermal Eng. 2023;**49**:103376*.

30 Suresh, S., Venkitaraj, K. P., Selvakumar, P., et al. ‘‘Effect of Al2O3–Cu/water hybrid nanofluid in heat transfer’’. *Exp Therm Fluid Sci. 2012;**38**:54-60*.

31 Labib, M. N., Nine, M. J., Afrianto, H., et al. ‘‘Numerical investigation on effect of base fluids and hybrid nanofluid in forced convective heat transfer’’. *Int J Therm Sci. 2013;**71**:163-171.*

32 Sundar, L. S., Sousa, A. C., Singh, M. K. ‘‘Heat transfer enhancement of low volume concentration of carbon nanotube-Fe3O4/water hybrid nanofluids in a tube with twisted tape inserts under turbulent flow’’. *J Therm Sci Eng Appl. 2015;**7**(2):021015.*

33 Nadeem, S., Abbas, N., Khan, A. U. ‘‘Characteristics of three-dimensional stagnation point flow of hybrid nanofluid past a circular cylinder’’. *Results Phys. 2018;**8**:829-835*.

34 Nadeem, S. and Abbas, N. ‘‘On both MHD and slip effect in micropolar hybrid nanofluid past a circular cylinder under stagnation point region’’. *Can J Phys. 2018; **97**(4), 392-399*.

35 Sheikholeslami, M., Jafaryar, M., Li, Z. ‘‘Nanofluid turbulent convective flow in a circular duct with helical turbulators considering CuO nanoparticles’’. *Int J Heat Mass Transfer. 2018;**124**:980-989*.

36 Dalkılıç, A. S., Türk, O. A., Mercan, H., et al. ‘‘An experimental investigation on heat transfer characteristics of graphite-SiO2/water hybrid nanofluid flow in horizontal tube with various quad-channel twisted tape inserts’’. *Int Commun Heat Mass Transfer. 2019;**107**:1-13.*

37 Sheikholeslami, M., Gerdroodbary, M. B., Moradi, R., et al. ‘‘Application of Neural Network for estimation of heat transfer treatment of Al2O3-H2O nanofluid through a channel’’. *Comput Methods Appl Mech Eng. 2019;**344**:1-12.*

38 Shah, Z., Rooman, M., Shutaywi, M. ‘‘Computational analysis of radiative engine oil-based Prandtl–Eyring hybrid nanofluid flow with variable heat transfer using the Cattaneo–Christov heat flux model’’. *RSC Adv. 2023;**13**(6):3552-3560.*

39 Noreen, S., Farooq, U., Waqas, H., et al. ‘‘Comparative study of ternary hybrid nanofluids with role of thermal radiation and Cattaneo-Christov heat flux between double rotating disks’’. *Sci Rep. 2023;**13**(1):7795*.

40 Ullah, A., Fatima, N., Alharbi, K. A. M., et al. ‘‘A Numerical Analysis of the Hybrid Nanofluid (Ag+ TiO2+ Water) Flow in the Presence of Heat and Radiation Fluxes’’. *Energies. 2023;**16**(3):1220*.

41 Rehman, A., Khun, M. C., Khan, D., et al. ‘‘Stability analysis of the shape factor effect of radiative on MHD couple stress hybrid nanofluid’’. *South Afr J Chem Eng. 2023;**46**:394-403*.

Author Biography

Dr. Nadeem Abbas: Dr. Nadeem Abbas completed his PhD at the Quaid I Azam University in Islamabad, Pakistan. He was working as an Assistant Professor at Riphah International University Faisalabad Campus, Faisalabad, Pakistan. He is highly cited and has published many articles in ISI highly impact factor journals. Now, he is working as a researcher at Prince Sultan University Saudi Arabia.

Prof. Dr. Wasfi Shatanawi: He was working as a full professor in the Department of Mathematics at Hashemite University, Jordon. Now, he is working as a full professor in the Department of Mathematics at Prince Sultan University, Riyadh, Saudi Arabia. According to clarivate analytic, Prof. Shatanawi was highly cited researcher for the years 2015, 2016, 2017 and 2018. Moreover, Prof. Shatanawi has been ranked as one of the top 2 of the highly cited scientist list created by Stanford University for the years 2019, 2020, 2021 2022. He also published many papers and achieved the Best Researcher award from Prince Sultan University.

Prof. Dr. Kamaleldin Abodayeh: He served as a full professor in the Department of Mathematics at Prince Sultan University in Riyadh, Saudi Arabia. In recognition of his scholarly contributions, he garnered substantial citations in the year 2023. His prolific research output includes numerous publications in high-impact factor journals indexed by ISI.

Notably, his exceptional achievements led to him being honored with the Best Researcher award from Prince Sultan University. His impactful work and dedication to advancing knowledge in the field are reflected not only in his extensive publication record but also in the recognition received from the academic community.

Prof. Dr. Taqi A. M. Shatnawi: He completed his Doctor of Philosophy from the School of Mathematical & Statistics at Carleton University. Now, he is working as a Professor in The Hashemite University Jordon. He has been named as a highly cited researcher.

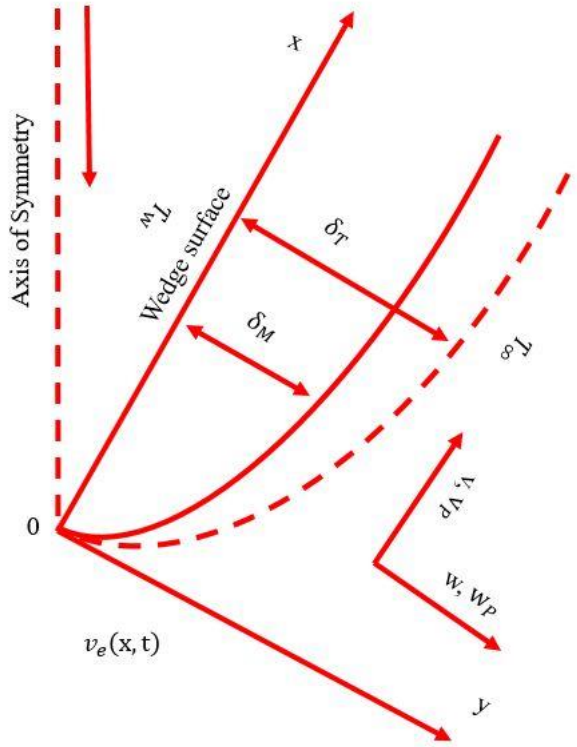

Fig. 1: Unsteady flow of hybrid nanofluid at wedge.

Table 1: Thermodynamics charactristics of nanoparticles and base fluid.

Thermo Physical Properties	MWCNT	SWCNT	Fluid Phase(water)
$C_p\left(J/kg\right)K$	796	425	4179
$\rho\left(\frac{kg}{m^3}\right)$	1600	2600	997.1
$k\left(\frac{W}{mK}\right)$	3000	6600	0.613

Table 2: computational analysis of physical parameter for skin friction and Nusselt number.

Φ_2	Ri	M	λ_1	ξ	λ	γ	K	ζ	Skin Friction	Nusselt Number
0.005	0.1	0.4	0.4	2.5	0.1	0.1	2.5	0.2	0.022924648	0.00013399082
0.02									0.025884106	0.000054466497

0.04									0.028719994	0.000010327846
0.06									0.030822679	-0.000008625752
0.02	0.1								0.025884106	0.000054466497
	0.2								0.026523473	0.000067191767
	0.3								0.027143696	0.000079502957
	0.4								0.027745664	0.000091419442
	0.1	0.2							0.024544164	0.000027690757
		0.4							0.025884106	0.000054466497
		0.6							0.027143696	0.000079502957
		0.8							0.028330203	0.00010295933
		0.4	0.2						0.024512273	0.000028220733
			0.4						0.025884106	0.000054466497
			0.6						0.02717562	0.000078784085
			0.8						0.028393921	0.000101350500
			0.4	2.0					0.026623413	0.000045084643
				2.5					0.025884106	0.000054466497
				3.0					0.025203738	0.000062859885
				3.5					0.024575794	0.000070406006
				2.5	0.1				0.025884106	0.000054466497
					0.2				0.012775416	0.00000016992533
					0.3				0.0072704799	-0.000020241404
					0.4				0.0048228432	-0.000021641566
					0.1	0.1			0.025884106	0.000054466497
						0.2			0.023404864	0.0000087829005
						0.3			0.021493004	-0.000011058396
						0.4			0.020004216	-0.000019422214
						0.1	2.0		0.025629085	0.000037483225
							2.5		0.025884106	0.000054466497
							3.0		0.026215294	0.000070269318
							3.5		0.026584075	0.000084924069
							2.5	0.2	0.025884106	0.000054466497
								0.3	0.021134284	0.000044471708
								0.4	0.018302827	0.000038513629
								0.5	0.016370546	0.000034447637

Table 3: Comperitive analysis of skin friction and Nusselt number with Hossain et al. [11] when $Pr = 0.72, Ri = 4.0, K = 0.0, \chi = 1.0, \lambda = 0.0, \gamma = 0.0, M = 0.0, \lambda_1 = 0.0, \Phi_1 = \Phi_2 = 0.0$.

ζ	Hossain et al. [11].	Present Results
0.010	32.33126	32.23678432
0.100	10.22307	10.13678941
0.500	4.55937	4.489512652
1.000	3.19704	3.078965831
2.000	2.19798	2.086974322
3.000	1.74511	1.678954327
4.000	1.50073	1.489706724
6.000	1.31603	1.267583450
8.000	1.26245	1.189657843

10.00	1.21931	1.123246572
15.00	1.18085	1.056785321
20.00	1.16491	1.023145874

Nomenclature

V,W	Velocity components, m/s	Ri	Richardson number
μ_{hnf}	Dynamic viscosity of hybrid nanofluid, kg/ms	μ_{nf}	dynamic viscosity of nanofluid, kg/ms
ν_{hnf}	Kinematic viscosity of hybrid nanoluid, m^2/s	ν_{nf}	kinematic viscosity of nanoluid, m^2/s
ρ_{hnf}	Density of hybrid nanofluid, kg/m^3	ρ_{nf}	Density of nanofluid, kg/m^3
α_{hnf}	Thermal diffusivity of hybrid nanofluid	α_{nf}	thermal diffusivity of nanofluid
k_{hnf}	Thermal conductivity of hybrid nanoflui	k_{nf}	Thermal conductivity of nanoflui
P	pressure, kg/ms^2	σ	Dimensionless parameter
$(\rho c_p)_{hnf}$	Heat capacitance of hybrid nanofluid	η	Dimensionless similarity variable
T	Temperature of the fluid	$(\rho c_p)_{nf}$	Heat capacitance of nanofluid
t	Dimensional time, s	M	Magnetic field
Nu	Nusselt number	Re	Reynolds number
Φ_1,Φ_2	Nanoparticles concentration	Pr	Prandtl number
w,v	Velocity components	ζ	Fluctuation factor
K	Dimensionless parameter	λ_1	Porosity parameter
γ	Thermal slip	λ	Velocity slip
$\overline{T}_0$	Surface temperature	$\overline{T}_\infty$	Ambient temperature

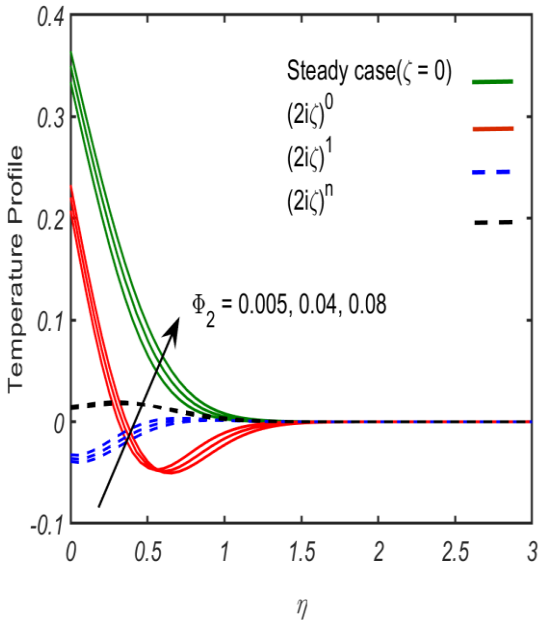

Fig. 2: Difference between temperature and Φ_2.

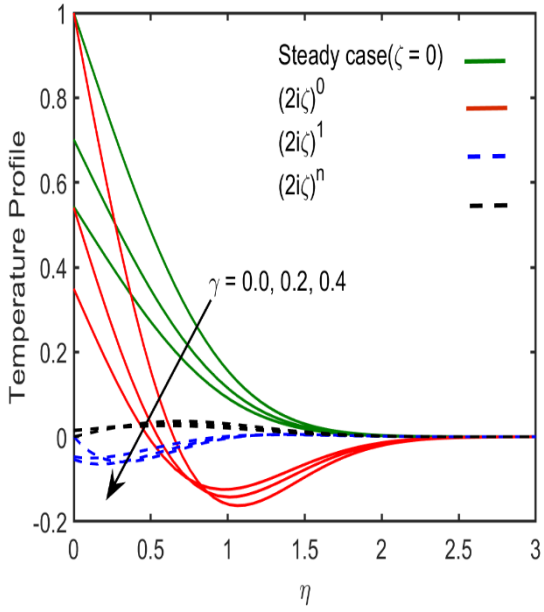

Fig. 3: Difference between temperature and γ.

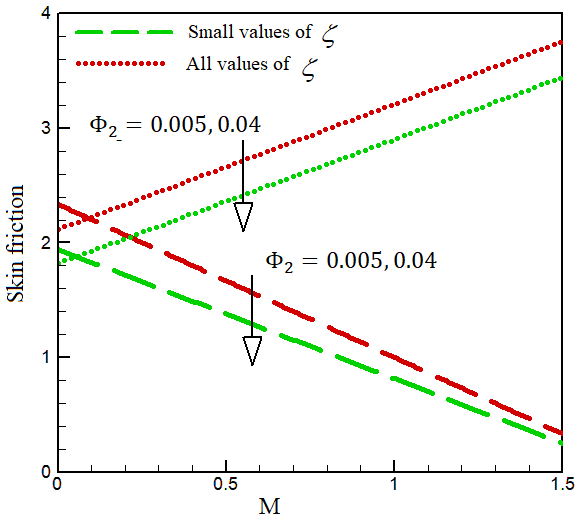

Fig. 4: Comparitive resulst of M and Φ_2 for Skin friction.

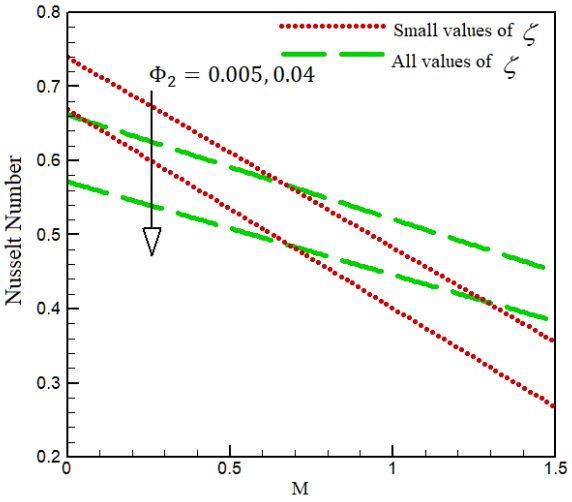

Fig. 5: Comparitive resulst of M and Φ_2 for Nusselt number.

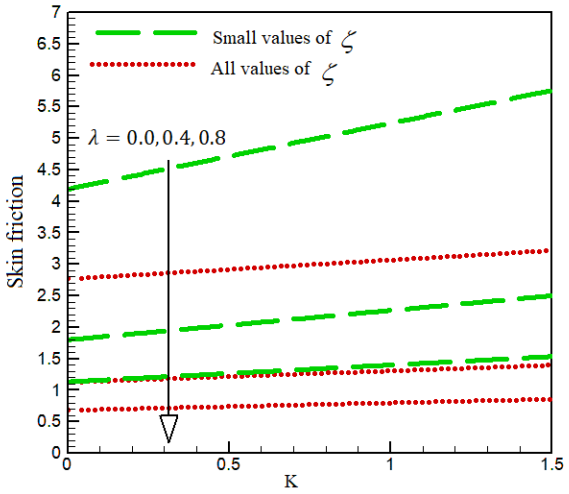

Fig. 6: Comparitive resulst of λ and K for Skin friction.

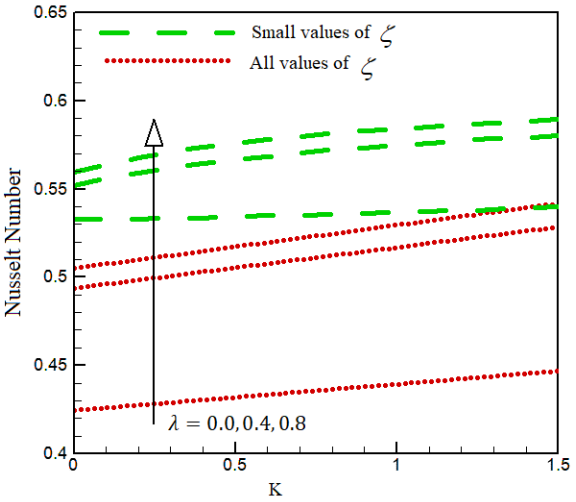

Fig. 7: Comparitive resulst of λ and K for Nusselt number.